Detecting Melanoma in Dermoscopy Images Using Scale Adaptive Local Binary Patterns

Farhan Riaz[1], Ali Hassan[1], Muhammad Younis Javed[1] and Miguel Tavares Coimbra[2]

***Abstract*— Recent advances in the area of computer vision has led to the development of various assisted diagnostics systems for the detection of melanoma in the patients. Texture and color are considered as two fundamental visual characteristics which are vital for the detection of melanoma. This paper proposes the use of a combination of texture and color features for the classification of dermoscopy images. The texture features consist of a variation of local binary pattern (LBP) in which the strength of the LBPs is used to extract scale adaptive patterns at each pixel, followed by the construction of a histogram. For color feature extraction, we used standard HSV histograms. The extracted features are concatenated to form a feature vector for an image, followed by classification using support vector machines. Experiments show that the proposed feature set exhibits good classification performance comparing favorably to other state-of-the-art alternatives.**

I. Introduction

Melanoma is considered one of the deadliest forms of skin cancer having a very high mortality rate [1]. The incidence rate for melanoma has been increasing over the past decade, making it one of the domains that has been attracting the attention of the cancer research community. It has been found that the early detection of melanoma in the patients can significantly increase the survival rates for the patients [2]. Dermoscopy is a clinical procedure, that is used by the dermatologists to diagnose the skin pathologies. It is a non-invasive procedure that is used for the *in vivo* observation of the skin lesions. In a dermoscopy procedure, the physicians apply gel to the skin of the patients and inspect the skin with a magnification instrument, known as *dermoscope* allowing the inspection of surface and sub-surface structures which are not visible to the naked eye [3]. The diagnosis of dermoscopy images is carried out using an assessment of these structures for which several medical rules have been defined, the most common of which are the ABCD rule, Menzies' method and the seven point check list [3]. Studies have shown that the application of these rules has resulted in an effective early detection of melanoma.

Assisted decision systems for the detection of melanoma can be constructed using these underlying rules which can be interpreted as visual features in computer vision. The ABCD rule investigates the asymmetry (A), border (B), color (C) and differential structures (D) of the lesion. The Menizes' method investigates two types of features in dermoscopy images: negative (symmetrical pattern, single color) and positive (blue-white veil, atypical dots and network etc.). The presence of positive features indicates the presence of melanoma. Finally, the seven point check-list indicates a score for the presence of a lesion. This check-list inspects the presence of differential structures in a lesion. It is important to note that the analysis of differential structures and color of the lesion are most common among these three sets of clinical rules motivating the computer vision researchers to propose adequate visual features for dermoscopic image analysis.

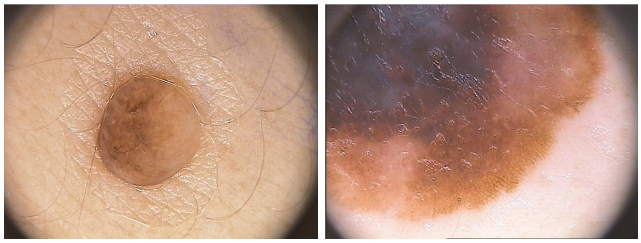

a). Normal Lesion b). Melanoma

Fig. 1: Dermoscopy images: The left figure shows a normal skin lesion whereas the right one indicates a melanoma.

In this paper, we intend to mimic the human classification of dermoscopy images using texture and color features from the images. The rest of the paper is organized as follows: we describe the visual features that have been used for feature extraction from dermoscopy images (Section II) followed by a description of the dataset used in this paper (Section III). Later, we present our experimental results (Section IV) followed by a discussion (Section V).

II. Methods

A. Local Binary Patterns (LBP)

The differential structures in dermoscopy images can be analyzed using the local binary pattern (LBP) texture descriptor. It unifies the structural and statistical information of the texture using a histogram of the LBP codes. It is a powerful local descriptor that has been widely used in various vision related applications [4]–[6]. Originally proposed by Ojala et al. [7], the LBP is a gray scale invariant texture descriptor that creates a pattern at every pixel in the image by thresholding its neighborhood with the value of the central pixel and concatenating the results binomially in the form of

*This work was supported by the National University of Sciences and Technology, Islamabad, Pakistan and the Instituto de Telecomunicações, Faculdade de Ciências da Universidade do Porto, Porto, Portugal and and Quadro de Referência Estratégica Nacional.

[1]F. Riaz, A. Hassan and M. Y. Javed are with the Department of Computer Engineering, National University of Sciences and Technology, Islamabad, Pakistan (e-mail: farhan.riaz, alihassan, myjaved@ceme.nust.edu.pk).

[2]M. Coimbra is with the Instituto de Telecomunicações, Department of Computer Science, Faculdade de Ciências da Universidade do Porto, 4169-007 Porto, Portugal (e-mail: mcoimbra@dcc.fc.up.pt).

978-1-4244-7929-0/14/$26.00 ©2014 IEEE

a number. The thresholding function for the most basic LBP can be obtained as follows:

$$LBP_{P,R} = \sum_{p=0}^{P-1} s(g_p - g_c)2^p,\ s(x) = \begin{cases} 1 & x \leq 0 \\ 0 & x > 0 \end{cases} \quad (1)$$

where g_c and g_p denote the gray level values of the central pixel and its neighbor respectively, and p is the index of the neighbor. P is the number of the neighbors in a circular set surrounding a pixel at a radius of R from g_c. Suppose that the coordinate g_c is $(0, 0)$, the coordinate of each neighboring pixel g_p is determined according to its index p and parameter (P, R) as $(R\cos(2\pi p/P), R\sin(2\pi p/P))$. The gray values of the neighbors that are not located at the image grids can be estimated by an interpolation operator. A parameter to quantify the uniformity of the LBP is defined as

$$U(LBP_{P,R}) = |s(g_{P-1} - g_c) - s(g_0 - g_c)| + \sum_{p=1}^{P-1} |s(g_p - g_c) - s(g_{p-1} - g_c)| \quad (2)$$

which corresponds to the number of spatial transitions (bitwise $0/1$ changes) in the pattern. The motivation for using uniform LBPs is their ability to detect the important intrinsic characteristics of textures like spots, line edges, edges and corners (Fig. 2).

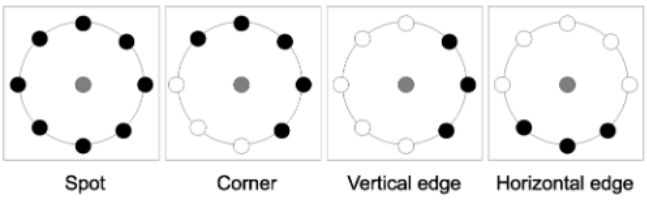

Fig. 2: Examples of different microstructures which are detected using LBP. The pixel in gray color indicates the center pixel g_c, the white pixels indicate the neighbors which are greater than g_c whereas the black pixels indicate the neighbors which are less than g_c (adapted from [8]).

B. Scale adaptive LBP based on local contrast

Standard LBPs typically quantize the difference between the center pixel and its neighbors. Although the LBPs capture the texture patterns in the images very effectively, an enhancement in the description of texture content can be obtained if the strengths of the LBPs are also taken into account. This is mainly because, image texture is not just characterized by the patterns which are available but also by the strength (local contrast) of the patterns. More specifically, the observers typically analyse the images with different levels of visual attention (detail) depending on the richness of texture content (contrast). Thus, an enhancement in the description of texture content can be obtained if the strength of LBPs is also incorporated in the texture descriptor.

To take the strength of LBPs into account, we have considered a novel methodology to use scale adaptive LBPs for feature extraction. The multiresolution LBPs can be obtained by varying the values of R to obtain the patterns at various radii from the center pixel. Let $r_1, r_2, ..., r_k$ be the radii at which the LBPs are calculated. At each pixel position, the absolute difference between the center pixel and its neighbors can be given as:

$$C^k(g_c) = \sum_{i=0}^{P-1} |g_p^k - g_c| \quad (3)$$

where $C^k(g_c)$ represents the strength of an underlying LBP at the resolution r_k. The LBP having the highest strength consists of the most relevant pattern and can be obtained as follows:

$$ULBP_{g_c} = \underset{C^k(g_c)}{\arg\max}\{ULBP(P, r_k)\} \quad (4)$$

Therefore, the LBP at g_c is represented by the pattern, which exhibits the maximum strength i.e., $C^k(g_c)$ when analysed at various resolutions at the pixel g_c.

C. Color descriptors

The standard RGB color space has several drawbacks: i). it is not perceptually uniform and ii). it exhibits a high correlation among the three constituent color channels. It is well known that there are some other color spaces which are designed to approximate the human visual system. For the extraction of color features from the images, we have employed one such space, known as the HSV (Hue, Saturation, Value) color space. In specific, we have used the HSV histograms for the calculation of color features.

To construct the HSV histograms we quantize H with 16 bins, S with 4 bins and V with 4 bins. This leads to a total of $16 \times 4 \times 4 = 256$ bins. Note that instead of concatenating the histograms of each color channel independently, we calculated the joint distribution of H, S and V channels giving us a a multivariate distribution (3-dimensional) of color features. These histograms have been widely used for color feature extraction and are an integral part of the MPEG-7 visual descriptors [9].

D. Dimensionality reduction

Feature extraction is followed by dimensionality reduction (DR). The need for DR is motivated by the fact that the dermoscopy images suffer from the problem of reduced color spaces and thus several bins (features) in the HSV histograms are expected to be empty. These features, if incorporated in for classification are expected to increase the computational load on the classifier. Therefore, we have used principal component analysis (PCA) for dimensionality reduction [10]. The PCA detects the variance structure in the data and identifies the directions along which the data subspace exhibits high variance. In our experiments, we have retained 95% variance in the data and used it for our classification experiments.

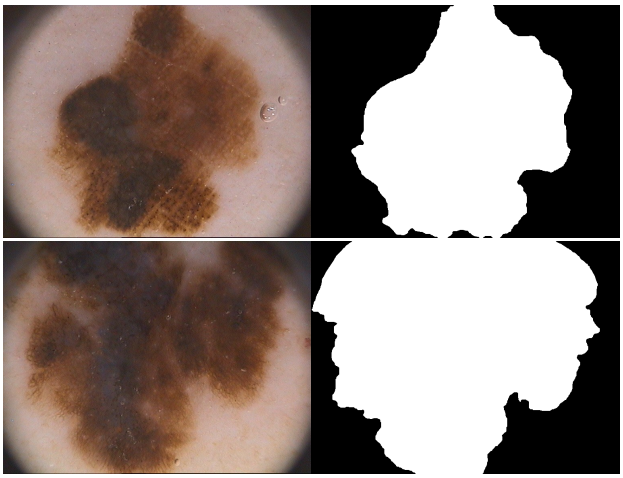

Fig. 3: Ground truth for dermoscopy: original image representing melanoma (left) and manually segmented mask of image region indicating melanoma (right).

E. Classification

For the purpose of classification, we have used support vector machines (SVM) [11]. An SVM classifier finds the hyperplane which maximizes the margin of separation between two distinct classes. Given a training set $X_{1...N}$ containing N training labeled samples and coefficients $\alpha_{1...N}$ learned in the training step, the decision function of SVM is as follows:

$$y(x) = \sum_i \alpha_i K(X_i, x) + b \tag{5}$$

where $K(.)$ is the kernel function and x is the input vector. In our implementation, we have used the linear kernel for SVM classification. The [1]weka data mining tool was used in our experiments [12]. All results were obtained using 10-fold cross validation.

III. Materials

The dataset that we have used is composed of 200 dermoscopy images with the following composition: 80% (160) nevus and 20% (40) melanoma. The images were acquired at the Hospital Pedro Hispano, Matosinhos [3]. All images have been acquired during clinical exams using a dermoscope at a magnification of 20x with a resolution of 765x573 pixels. Each image was manually segmented (to identify the lesions) and classified by an experienced dermatologist as being normal, atypical nevus (benign) or melanoma (malignant).

IV. Experimental results

For our classification experiments, we have used only the manually annotated image regions (Fig. 3). The objective of the classification task is to identify the presence of melanoma in the patients labelling each observation as either a *nevus* or *melanoma*. The feature extraction is followed by classification using SVMs with linear kernel and 10-fold cross validation. For the extraction of LBPs are multiple resolutions in the underlying methodology, we have used the radii of 1.0, 1.5 and 2.0 and at each resolution, 8 neighbors were considered. To assess the performance of the underlying features used in this paper, three different experiments were performed:

[1]http://www.cs.waikato.ac.nz/ml/weka/

A. Experiment 1

In the first experiment, our objective was to assess the performance of texture features for the classification of dermoscopy images. For performing this comparison, we selected the most popular texture features (T1 - Proposed scale adaptive LBP; T2 - LBP [13]; T3 - autocorrelation homogeneous texture [14]; T4 - homogeneous texture; T5 - wavalet subband statistics). Our results show that the proposed texture feature (T1) set outperforms the other texture descriptors that have been considered in this paper. The AHT features (T3), although being rotation and scale invariant, do not show good performance as compared to T1 giving low sensitivity to the detection of melanoma. We attribute the superior performance of T1 to its ability to capture the micro-structures in the images which are effectively representative of the differential structures in the images which are considered as clinically relevant for the classification of melanoma. The scale adaptation in T1 approximates the human observers (clinicians) who try to visualize the image texture at various levels of attention, giving superior classification results in the identification of melanoma. Additionally, T1 is also invariant to the illumination variations (homogeneous and non-homogeneous) in the images (unlike Gabor filter based features) giving us better results in the identification of melanoma.

TABLE I: Overall classification accuracy for the detection of melanoma when texture features are used for feature extraction.

Methods	Sensitivity	Specificity
T1	**0.82**	**0.88**
T2	0.75	0.87
T3	0.79	0.88
T4	0.64	0.86
T5	0.61	0.85

B. Experiment 2

This experiment was conducted to assess the empirical performances of histograms obtained from different color spaces (C1 - HSV histograms; C2 - RGB histograms). Our experiments show that the HSV histograms show the better performance as compared to the histograms obtained from the RGB color spaces.

C. Experiment 3

Last but not the least, this experiment deals with a concatenation of color and texture features followed by dimensionality reduction for input to the statistical classifiers. We have obtained several combinations of texture and color features

TABLE II: Overall classification accuracy for the detection of melanoma when color features are used for feature extraction.

Methods	Sensitivity	Specificity
C1	**0.77**	**0.85**
C2	0.70	0.63

which were relevant for this study. The best performance was obtained when a combination of the proposed scale adaptive texture features was used with the HSV histograms (Table III). For all combinations of features presented in this paper, the use of color and texture features results in a performance enhancement in the classification of melanoma. The worst performance is given by the non-invariant texture descriptors (wavelets and HT).

TABLE III: Overall classification accuracy for the detection of melanoma when color and texture features are concatenated to form a descriptor for an underlying lesion.

Methods	Sensitivity	Specificity
T1+C1	**0.84**	**0.94**
T1+C2	0.83	0.88
T2+C1	0.80	0.90
T3+C1	0.83	0.91
T4+C1	0.67	0.90
T5+C1	0.69	0.86

V. Discussion

This paper deals with a study on the visual descriptors for dermoscopy images. Clinical findings have concluded that color and texture are two most vital visual characteristics which are necessary for the quantification of melanoma in the patients. For the purpose of feature extraction in this paper, we have used the HSV histograms for color feature extraction. For the description of differential structures in the images, we have proposed a variant of local binary patterns that selects scale adaptive LBP based on the strengths of the underlying LBPs calculated at various resolutions. A comparison of the these features with other state-of-the-art texture descriptors is presented individually, and as their combination with the HSV histograms. The results have shown good performance for the proposed texture descriptor as compared to other methods.

Although good results are obtained, it is evident that the color histograms are limited as they quantise the color spaces in equal intervals. Since the dermoscopy images suffer from reduced color spaces, therefore more adequate color descriptors can be constructed by adapting the color spaces to the specific scenario of dermoscopy potentially giving better results for the identification of melanoma.

Acknowledgements

This paper was financially supported by National University of Sciences and Technology (NUST) Islamabad, Instituto de Telecomunicações, Faculdade de Ciências da Universidade do Porto, Porto, Portugal (GEMINI: PEST-OE/EEI/LA0008/2013) and Quadro de Referência Estratégica Nacional (I-City for Future Health: NORTE-07-0124-FEDER-000068). We would like to thank all the funding entities for providing vital financial assistance for carrying out this research. We are also thankful to the Hospital Pedro Hispano, Porto, Portugal for collecting the valuable dermoscopy data and making it available online for research.

References

[1] J. F. Alcón, C. Ciuhu, W. Ten Kate, A. Heinrich, N. Uzunbajakava, G. Krekels, D. Siem, and G. de Haan, "Automatic imaging system with decision support for inspection of pigmented skin lesions and melanoma diagnosis," *Selected Topics in Signal Processing, IEEE Journal of*, vol. 3, no. 1, pp. 14–25, 2009.

[2] I. Maglogiannis and C. N. Doukas, "Overview of advanced computer vision systems for skin lesions characterization," *Information Technology in Biomedicine, IEEE Transactions on*, vol. 13, no. 5, pp. 721–733, 2009.

[3] C. Barata, M. Ruela, M. Francisco, T. Mendonça, and J. S. Marques, "Two systems for the detection of melanomas in dermoscopy images using texture and color features," *IEEE Systems Journal*, 2013.

[4] A. Sousa, M. Dinis-Ribeiro, M. Areia, and M. Coimbra, "Identifying cancer regions in vital-stained magnification endoscopy images using adapted color histograms," in *Image Processing (ICIP), 2009 16th IEEE International Conference on*, pp. 681–684, IEEE, 2009.

[5] B. Li and M.-H. Meng, "Computer-aided detection of bleeding regions for capsule endoscopy images," *Biomedical Engineering, IEEE Transactions on*, vol. 56, pp. 1032–1039, April 2009.

[6] L. Sorensen, S. Shaker, and M. de Bruijne, "Quantitative analysis of pulmonary emphysema using local binary patterns," *Medical Imaging, IEEE Transactions on*, vol. 29, pp. 559–569, Feb 2010.

[7] T. Ojala, M. Pietikainen, and T. Maenpaa, "Multiresolution gray-scale and rotation invariant texture classification with local binary patterns," *Pattern Analysis and Machine Intelligence, IEEE Transactions on*, vol. 24, no. 7, pp. 971–987, 2002.

[8] L. Sorensen, S. Shaker, and M. de Bruijne, "Quantitative analysis of pulmonary emphysema using local binary patterns," *Medical Imaging, IEEE Transactions on*, vol. 29, pp. 559–569, Feb 2010.

[9] B. S. Manjunath, J.-R. Ohm, V. V. Vasudevan, and A. Yamada, "Color and texture descriptors," *Circuits and Systems for Video Technology, IEEE Transactions on*, vol. 11, no. 6, pp. 703–715, 2001.

[10] I. Jolliffe, *Principal component analysis*. Wiley Online Library, 2005.

[11] I. Guyon, J. Weston, S. Barnhill, and V. Vapnik, "Gene selection for cancer classification using support vector machines," *Machine learning*, vol. 46, no. 1-3, pp. 389–422, 2002.

[12] M. Hall, E. Frank, G. Holmes, B. Pfahringer, P. Reutemann, and I. H. Witten, "The weka data mining software: an update," *ACM SIGKDD explorations newsletter*, vol. 11, no. 1, pp. 10–18, 2009.

[13] T. Mäenpää, *The Local binary pattern approach to texture analysis: Extenxions and applications*. Oulun yliopisto, 2003.

[14] F. Riaz, F. B. Silva, M. D. Ribeiro, and M. T. Coimbra, "Invariant gabor texture descriptors for classification of gastroenterology images," *Biomedical Engineering, IEEE Transactions on*, vol. 59, no. 10, pp. 2893–2904, 2012.